3.10 A COMBINATION OF EMPIRICAL ORTHOGONAL FUNCTION AND NEURAL NETWORK APPROACHES FOR PARAMETERIZING NONLINEAR INTERACTIONS IN WIND WAVE MODELS.

Vladimir M. Krasnopolsky *, Hendrik L. Tolman, and Dmitry V. Chalikov
Science Applications International Corp. at the National Centers for Environmental Predictions

1. INTRODUCTION

Ocean wind wave modeling for hindcast and forecast purposes has been at the center of interest for many decades. Numerical prediction models are generally based on a form of the spectral energy or action balance equation

$$\frac{DF}{Dt} = S_{in} + S_{nl} + S_{ds} + S_{sw} \qquad (1)$$

where F is the spectrum, S_{in} is the input source term, S_{nl} is the nonlinear interaction source term, S_{ds} is the dissipation or 'whitecapping' source term, and S_{sw} represents additional shallow water source terms. Several studies (Hasselman et al 1973) identified the active role of the nonlinear interactions in wave growth and the need for explicit modeling of S_{nl} in wave models. State-of-the-art or so-called third generation wave models therefore explicitly model this source term.

In its full form (e.g., Hasselmann and Hasselmann 1985), the calculation of the interactions S_{nl} requires the integration of a six-dimensional Bolzmann integral:

$$S_{nl}(\vec{k}_4) = T \otimes F(\vec{k}) =$$
$$= \omega_4 \int G(\vec{k}_1,\vec{k}_2,\vec{k}_3,\vec{k}_4)\cdot\delta(\vec{k}_1+\vec{k}_2-\vec{k}_3-\vec{k}_4)\cdot\delta(\omega_1+\omega_2-\omega_3-\omega_4)$$
$$\times [n_1\cdot n_3\cdot(n_4-n_2)+n_2\cdot n_4\cdot(n_3-n_1)]d\vec{k}_1\,d\vec{k}_2\,d\vec{k}_3$$
$$n(\vec{k}) = \frac{F(\vec{k})}{\omega}; \qquad \omega^2 = g\cdot k\cdot\tanh(kh) \qquad (2)$$

where the complicated coupling coefficient G contains moving singularities (K. Hasselmann 1973). This integration requires roughly 10^3 to 10^4 times more computational effort than all other aspects of the wave model combined. Present operational constraints require that the computational effort for the estimation of S_{nl} should be of the same order of magnitude as the remainder of the wave model. This requirement was met with the development of the Discrete Interaction Approximation (DIA, Hasselman et al 1985). The development of the DIA allowed for the successful development of the first third-generation wave model WAM (WAMDI Group 1988). More than a decade of experience with the WAM model and its derivatives has identified shortcomings of the DIA. The DIA tends to unrealistically increase the directional width of spectra, has a systematic spurious impact on the shape of the spectrum near the spectral peak frequency, and has a much too strong signature at high frequencies. In present third generation wave models, these deficiencies can be countered at least in part by the dissipation source term S_{ds}, which is generally used for tuning the energy balance in the equation (1). Although this approach gives good results, it is counterproductive, because it prohibits development of dissipation source terms based on solid physical considerations. With our increased understanding in the physics of wave generation and dissipation, this becomes an even bigger obstacle impeding further development of third-generation wave models.

2. NN PARAMETERIZATION OF S_{nl}

Considering the above, it is of crucial importance for the development of third generation wave models to develop *an economical yet accurate approximation* for S_{nl}. Here, we explore a Neural Network Interaction Approximation (NNIA) to achieve this goal (see also Krasnopolsky et al 2002). NNs can be applied here because the nonlinear interaction (2) is essentially a nonlinear mapping (symbolically represented in eq. (2) by T) which relates two vectors (2-D fields in this case). Thus, the nonlinear interaction source term can be considered as a nonlinear mapping between a spectrum F and a source term S_{nl}

$$S_{nl} = T(F)\ , \qquad (3)$$

where T is the exact nonlinear operator given by the full Bolzmann interaction integral (2) (Hasselmann and Hasselmann 1985). Discretization of S and F (as is necessary in any

* *Corresponding author address:* Vladimir Krasnopolsky, SAIC at EMC/NCEP/NOAA, 5200 Auth Rd., Camp Spring, MD 20906, e-mail: Vladimir.Krasnopolsky@noaa.gov
MMAB Contribution No. 224

numerical approach) reduces (3) to continuous mapping of two vectors of finite dimensions. Modern high resolution wind wave models use descretization on a two dimensional grid which leads to dimensions of S and F vectors of order of N (~1000) (Tolman 1999). It seems unreasonable to develop a NN approximation of such a high dimensionality (about 1000 inputs and outputs). Moreover, such a NN will be grid dependent.

In order to reduce the dimensionality of the NN and convert the mapping (3) to a continuous mapping of two finite vectors independent on the actual spectral discretization, the spectrum F and source function S_{nl} are expanded using systems of two-dimensional functions each of which (Φ_i and Ψ_q) creates a complete and orthogonal two-dimensional basis

$$F \approx \sum_{i=1}^{n} x_i \Phi_i, \quad S_{nl} \approx \sum_{q=1}^{m} y_q \Psi_q, \tag{4}$$

where for x_i and y_q we have

$$x_i = \iint F \Phi_i, \quad y_q = \iint S_{nl} \Psi_q \tag{5}$$

where the double integral identifies integration over the spectral space. Because both sets of basis functions $\{\Phi_i\}_{i=1,\ldots,n}$ and $\{\Psi_q\}_{q=1,\ldots,m}$ are complete, increasing n and m in (4) improves the accuracy of approximation, and any spectrum F and source function S_{nl} can be approximated by (4) with a required accuracy. Substituting (4) into Eq. (3) we can get

$$\boldsymbol{Y} = T(\boldsymbol{X}), \tag{6}$$

which represents a continuous mapping of the finite vectors $X \in \Re^n$ and $Y \in \Re^m$, and where T still represents the full nonlinear interaction operator. This operator can be approximated with a NN with n inputs and m outputs and k neurons in the hidden layer

$$\boldsymbol{Y} = T_{NN}(\boldsymbol{X}) \tag{7}$$

The accuracy of this approximation (T_{NN}) is determined by k, and can generally be improved by increasing k.

To train the NN approximation T_{NN} of T, a training set has to be created that consists of pairs of vectors $\boldsymbol{X}$ and $\boldsymbol{Y}$. To create this training set, a representative set of spectra F_p has to be generated with corresponding (exact) interactions $S_{nl,p}$ using eq. (2). For each pair $(F, S_{nl})_p$, the corresponding vectors $(\boldsymbol{X},\boldsymbol{Y})_p$ are determined using eq. (5). These pairs of vectors are then used to train the NN to obtain T_{NN}. After T_{NN} has been trained, the resulting NN Interaction Approximation (NNIA) algorithm consists of three steps:

1. decompose the input spectrum, F, by applying Eq. (5) to calculate $\boldsymbol{X}$;
2. estimate $\boldsymbol{Y}$ from $\boldsymbol{X}$ using Eq. (7);
3. compose the output source function, S_{nl}, from $\boldsymbol{Y}$ using Eq. (4).

A graphical representation of the NNIA algorithm is shown in Figure 1.

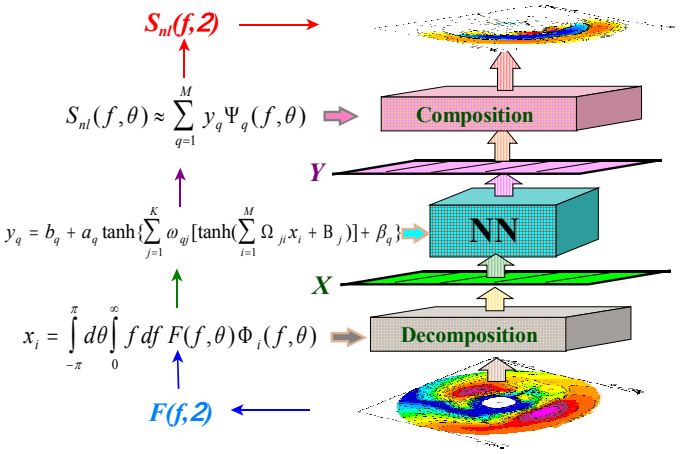

Figure 1. Graphical representation of the NNIA algorithm.

The above describes the general procedure for developing an NNIA. Development of an actual NNIA requires the following steps: (1) select basis functions Φ_i and Ψ_q and the number of each (n,m); (2) design a NN topology (number of neurons k); (3) construct a representative training set; and (4) select training strategies.

The first three points all have a significant impact on both accuracy and economy of a NNIA. Unfortunately, there is no pre-defined way to tackle these issues. It is therefore unavoidable that the development of a NNIA involves much iteration. The first requirement for a NNIA to be potentially useful in operational wave modeling is that the exact interactions S_{nl} are closely reproduced for computational costs comparable to that of the DIA.

In (Krasnopolsky et al, 2002) we address the basic feasibility of a NNIA, we have considered a NNIA to estimate the nonlinear interactions $S_{nl}(f,\theta)$ as a function of frequency f and direction θ from the corresponding spectrum $F(f,\theta)$. In this study we used a mathematical bases for the decomposition of the

nonlinear interactions $S_{nl}(f,\theta)$ and the spectra $F(f,\theta)$. As is common in parametric spectral descriptions, we choose separable basis functions where frequency and angular dependence are separated. For Φ_i this implies:

$$\Phi_i(f,\theta) \Rightarrow \Phi_{ij} = \phi_{f,i}(f)\phi_{\theta,j}(\theta) \qquad (8)$$

A similar separation was used for Ψ_q.

To train and test this NNIA, we used a set of about 10,000 simulated realistic spectra for $F(f,\theta)$, and the corresponding exact estimates of $S_{nl}(f,\theta)$ (Van Vledder et al 2000). Separate data sets have been generated for training and validation. Preliminary version of the NNIA algorithm (Krasnopolsky et al., 2002) has twice better accuracy than DIA and is only about 5 times slower than the DIA algorithm.

The results presented in this work represent the next stage of the development. To improve the accuracy of the NN algorithm, we attempted to optimize the basis used for the composition and decomposition of $F(f,\theta)$ and $S_{nl}(f,\theta)$. To guarantee the fastest conversions, we used a natural basis of empirical orthogonal functions (EOF) generated by the ensembles of spectra and nonlinear interactions correspondingly. In this case the basis functions are 2-D fields, the composition and decomposition procedures are straightforward (do not include Fourier transform). They converge faster and provide higher approximation accuracy than in the case of a mathematical basis (8). Table 1 shows comparison of accuracies of approximation using these two bases. EOF allow significantly more accurate approximation (approximately five times lower RMSE) for both $F(f,\theta)$ and $S_{nl}(f,\theta)$. The difference between CRMSE and Mean RMSE is explained below.

Table 1. RMSE approximation statistics for independent set of 10,000 F and S_{nl} comparing mathematical (Math) and EOF bases.

	Basis Type	CRMSE	Mean RMSE
F	**Math**	0.14	0.012
	EOF	0.03	0.0044
S_{nl}	**Math**	5,175.	425.
	EOF	623.	32.

To generate EOFs and to train this new NN, we simulated a set of 10,000 realistic spectra for $F(f,\theta)$, and the corresponding exact estimates of $S_{nl}(f,\theta)$ (Van Vledder et al 2000). Separate data set (10,000 spectra and nonlinear interactions) have been generated for test and validation. To distinguish our new NN algorithm based on the use of EOF from the previous one (NNIA), we will call it NNIAEOF. Table 2 compares the accuracy of DIA, NNIA, and NNIAEOF on the same independent (not used for training and/or generating of EOF bases) set of 10,000 F and S_{nl}. Two types of statistics are presented here. First is a cumulative RMSE which is calculated as,

$$CRMSE = \sqrt{\frac{\iint df d\theta \sum_{i=1}^{N} (X_i(f,\theta) - Y_i(f,\theta))^2}{N}} \qquad (9)$$

where N = 10,000, X_i is DIA or NNIA or NNIAEOF approximation for i-th $S_{nl}(f,\theta)$ and Y_i is the exact i-th S_{nl}. Second type of statistics presented in Table 2 are Mean RMSE and SD RMSE. RMSE is calculated for each particular nonlinear interaction in this case. Then the mean value and the standard deviation (SD) are calculated for this set of RMSEs.

Table 2. CRMSE, Mean RMSE and SD RMSE statistics for independent set of 10,000 F and S_{nl} comparing performances of DIA, NNIA, and NNIAEOF.

Method	CRMSE	Mean RMSE	SD RMSE
DIA	13,266.	3,124	5,273.
NNIA	6,590.	882.	1,888
NNIAEOF	2,836.	354.	750.

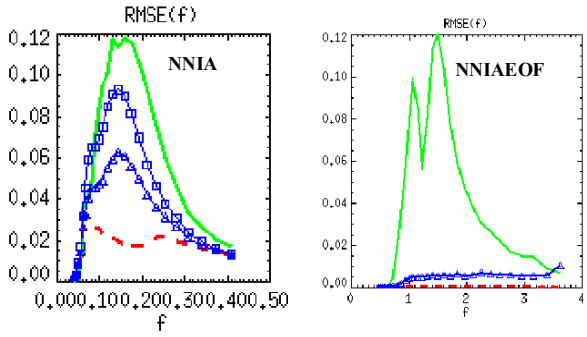

Figure 2. RMSEs as functions of frequency, f, for DIA (green), NNIA (blue, left panel, two blue curves correspond to different numbers of neurons in the hidden layer of the NN), and NNIAEOF (blue, right panel). Red curves show RMSEs of the approximation for Math basis (right panel) and EOF basis (left panel).

Table 2 demonstrates better performance of the NNIAEOF algorithm as compared with both DIA and NNIA. Figure 2 gives a graphical representation of this comparison. It also shows

a dramatic improvement in the accuracy of the approximation with the transition from the mathematical basis to the EOF basis. Figure 3 demonstrates a comparison of performances of DIA and NNIAEOF for different spectra (spectra with the different energy).

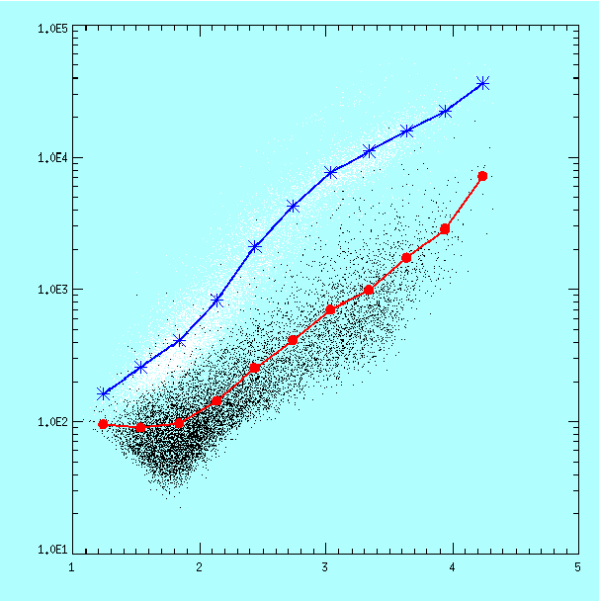

Figure 3. Comparison of performance (log_{10}(RMSE) along the vertical axis) of DIA (blue curve) and NNIAEOF (red curve) for different energies of the input spectra (horizontal axis).

Fig. 3 shows that advantage of the NNIAEOF algorithm as compared with DIA increases from the factor about 2 at low energies to about 10 at higher energies. Figure 4 shows a typical nonlinear interaction, S_{nl}, together with its representation by DIA and NNIAEOF.

3. CONCLUSIONS

In this study we showed that the use of EOF bases for the decomposition and composition of spectra and nonlinear interactions in a combination with the NN, which is trained to provide the relationship between the coefficients of these decompositions, gives significant advantage as compared with the use of mathematical bases. Transition from mathematical bases to natural bases (EOF) improved performance of our NN approach, NNIAEOF, about three times as compared with its previous version, NNIA. NNIAEOF five times outperforms DIA on average. For spectra of higher energy the improvement in accuracy reaches an order of magnitude. NNIA is still as

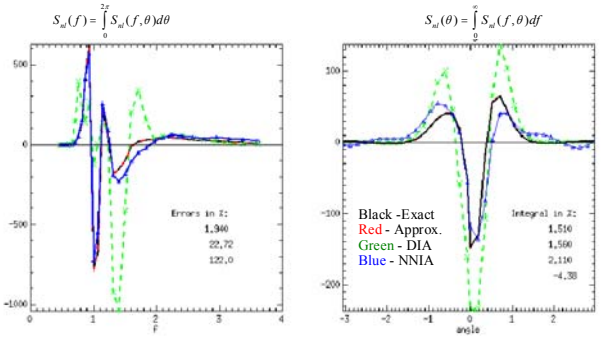

Figure 4. A typical nonlinear interaction (black) together with its the EOF approximation (red), DIA (green), and NNIAEOF (blue). Left panel shows S_{nl} integrated over the angle and right one shows S_{nl} integrated over the frequency.

fast as NNIA – several orders of magnitude faster than exact calculations and only four – five times slower than DIA.

We demonstrated that the use of a natural basis like EOF can improve the performance of our algorithm as compared with the case when a mathematical basis is used. We expect that a transition to a physical basis for decomposing S_{nl}, basis, which takes into account conservation laws, symmetries, and normalization, will allow us to further improve the performance of our NN approach.

References.

Hasselmann, K. et al. (1973) Measurements of wind-wave growth and swell decay during the Joint North Sea Wave Project (JONSWAP). Ergänzungshelf zur Deutschen Hydrographischen Zeitschrift, Reihe A (8) Nr.12, 95 pp.

Hasselmann, S. and K. Hasselmann (1985) Computations and parametrizations of the nonlinear energy transfer in a gravity wave spectrum. Part I: a new method for efficient computations of the exact nonlinear transfer integral, *Journal of Physical Oceanography*, pp. 1369-77.

Krasnopolsky, V.M., D.V. Chalikov, H.L. Tolman (2002) "A Neural Network Technique to Improve Computational Efficiency of Numerical Oceanic Models", *Ocean Modelling*, v. 4, 363-383

Tolman, H. L. (1999) User manual and system documentation of WAVEWATCH-III version 1.18, NOAA / NWS / NCEP /OMB technical note 166, 110 pp.

Van Veldder et al. (2000) Modelling of nonlinear quadruplet wave-wave interactions in operational coastal wave models, Abstract, accepted for presentation at ICCE 2000, Sydney .

WAMDI Group (1988) The WAM model - a third generation ocean wave prediction model, *Journal of Physical Oceanography*, 18, pp. 1775-1810.